

EPJ manuscript No.
(will be inserted by the editor)

Jet Tomography Studies in $AuAu$ Collisions at RHIC Energies

G.G. Barnaföldi^{1,2}, P. Lévai¹, G. Papp³, G. Fái⁴, and M. Gyulassy⁵

¹ RMKI KFKI, P.O. Box 49, Budapest 1525, Hungary

² Lab. for Information Technology, Eötvös University, Pázmány P. 1/A, Budapest 1117, Hungary

³ Dept. for Theoretical Physics, Eötvös University, Pázmány P. 1/A, Budapest 1117, Hungary

⁴ CNR, Kent State University, Kent, OH 44242, USA

⁵ Dept. of Physics, Columbia University, 538 W. 120th Street, New York, NY 10027, USA

the date of receipt and acceptance should be inserted later

Abstract. Recent RHIC results on pion production in $AuAu$ collision at $\sqrt{s} = 130$ and 200 AGeV display a strong suppression effect at high p_T . This suppression can be connected to final state effects, namely jet energy loss induced by the produced dense colored matter. Applying our pQCD-based parton model we perform a quantitative analysis of the measured suppression pattern and determine the opacity of the produced deconfined matter.

PACS. 12.38.Mh Quark-gluon plasma in quantum chromodynamics – 24.85+p Quarks, gluons, and QCD in nuclei and nuclear processes – 25.75-q Relativistic heavy-ion collisions

1 Introduction

The experimental data on high- p_T π^0 production in central $AuAu$ collisions at mid-rapidity at $\sqrt{s} = 130$ and 200 AGeV have shown a strong suppression compared to binary scaled pp data [1, 2]. This suppression vanishes with increasing centrality and no effect appears in peripheral $AuAu$ collisions. Thus a detailed quantitative analysis of the suppression pattern (“jet tomography” [3]) yields information about the properties of the produced dense matter and the impact parameter dependence of the formation of deconfined matter in $AuAu$ collisions. Recent data on dAu collisions [4, 5] validate our effort: since no suppression was found at mid-rapidity in the dAu reaction, initial state effects (e.g. a strong modification in the internal parton structure of the accelerated Au nuclei) can not be responsible for the measured suppression in $AuAu$ collisions. Thus, induced jet-energy loss in the final state becomes a strong candidate to explain the missing pion yield. Jet energy loss can be calculated in a perturbative quantum chromodynamics (pQCD) frame [6, 7].

We investigate jet energy loss in a pQCD improved parton model. In Sect. 2 we introduce the basis of our model, especially a phenomenological intrinsic transverse momentum distribution (intrinsic k_T) for the colliding nucleons, which is necessary to reach a better agreement between data and calculations in pp collisions [8, 9, 10, 11]. For nucleus-nucleus (AA) collisions, initial state effects are considered, e.g. nuclear multiple scattering, saturation in the number of semihard collisions, and a weak shadowing effect inside the nucleus [9, 10]. In Sect. 3 we summarize the description of induced gluon radiation in thin non-

Abelian matter and include the GLV-description [7] of energy loss into the pQCD improved parton model. This way our model becomes capable to extract the opacity values of the produced colored matter at different centralities. In Sect. 4 we discuss the obtained results.

2 Initial State Effects in $AuAu$ Collisions

The invariant cross section of pion production in an AA' collision can be described in a pQCD-improved parton model developed for pp collision and extended by a Glauber-type collision geometry and initial state nuclear effects for AA' collisions as [13, 14, 12]:

$$\begin{aligned}
 E_\pi \frac{d\sigma_\pi^{AA'}}{d^3p} &= \int d^2b d^2r t_A(r) t_{A'}(|\mathbf{b} - \mathbf{r}|) \frac{1}{s} \sum_{abc} \times \\
 &\times \int_{vw/z_c}^{1-(1-v)/z_c} \frac{d\hat{v}}{\hat{v}(1-\hat{v})} \int_{vw/\hat{v}z_c}^1 \frac{d\hat{w}}{\hat{w}} \int^1 dz_c \times \\
 &\times \int d^2\mathbf{k}_{Ta} \int d^2\mathbf{k}_{Tb} f_{a/A}(x_a, \mathbf{k}_{Ta}, Q^2) f_{b/A'}(x_b, \mathbf{k}_{Tb}, Q^2) \\
 &\times \left[\frac{d\hat{\sigma}}{d\hat{v}} \delta(1-\hat{w}) + \frac{\alpha_s(Q_r)}{\pi} K_{ab,c}(\hat{s}, \hat{v}, \hat{w}, Q, Q_r, \tilde{Q}) \right] \times \\
 &\times \frac{D_c^\pi(z_c, \tilde{Q}^2)}{\pi z_c^2}. \tag{1}
 \end{aligned}$$

Here $t_A(b) = \int dz \rho_A(b, z)$ is the nuclear thickness function normalized as $\int d^2b t_A(b) = A$. For small nuclei we use a sharp sphere approximation, while for larger nuclei the Wood-Saxon formula is applied.

In our next-to-leading order (NLO) calculation [12], $d\hat{\sigma}/d\hat{v}$ represents the Born cross section of the partonic subprocess and $K_{ab,c}(\hat{s}, \hat{v}, \hat{w}, Q, Q_r, \tilde{Q})$ is the corresponding higher order correction term, see Ref.s [12, 13, 14]. We fix the factorization and renormalization scales and connect them to the momentum of the intermediate jet, $Q = Q_r = (4/3)p_q$ (where $p_q = p_T/z_c$), reproducing pp data with high precision at high p_T [15].

The approximate form of the 3-dimensional parton distribution function (PDF) is the following:

$$f_{a/p}(x_a, \mathbf{k}_{T_a}, Q^2) = f_{a/p}(x_a, Q^2) \cdot g_{a/p}(\mathbf{k}_{T_a}). \quad (2)$$

Here, the function $f_{a/p}(x_a, Q^2)$ represents the standard longitudinal NLO PDF as a function of momentum fraction of the incoming parton, x_a at scale Q (in the present calculations we use the MRST(cg)[16] PDFs). The partonic transverse-momentum distribution in 2 dimensions, $g_{a/p}(\mathbf{k}_T)$, is characterized by an "intrinsic k_T " parameter as in Ref.s [10, 12]. In our phenomenological approach this component is described by a Gaussian function [10, 11].

Nuclear multiscattering is accounted for through broadening of the incoming parton's transverse momentum distribution function, namely an increase in the width of the Gaussian:

$$\langle k_T^2 \rangle_{pA} = \langle k_T^2 \rangle_{pp} + C \cdot h_{pA}(b). \quad (3)$$

Here, $\langle k_T^2 \rangle_{pp} = 2.5 \text{ GeV}^2$ is the width of the transverse momentum distribution of partons in pp collisions [10, 15], $h_{pA}(b)$ describes the number of *effective* NN collisions at impact parameter b , which impart an average transverse momentum squared C . The effectivity function $h_{pA}(b)$ can be written in terms of the number of collisions suffered by the incoming proton in the target nucleus. In Ref. [10] we have found a limited number of semihard collisions, $\nu_m = 4$ and the value $C = 0.4 \text{ GeV}^2$.

We take into account the isospin asymmetry by using a linear combination of p and n PDFs. The applied PDFs are also modified inside nuclei by the "shadowing" effect [17].

The last term in the convolution of eq. (1) is the fragmentation function (FF), $D_c^\pi(z_c, \tilde{Q}^2)$. This gives the probability for parton c to fragment into a pion with momentum fraction z_c at fragmentation scale $\tilde{Q} = (4/3)p_T$. We apply the KKP parametrization [18].

3 Jet-Quenching as a Final State Effect

The energy loss of high-energy quark and gluon jets traveling through dense colored matter is able to give information on the density of gluons [3]. This non-Abelian radiative energy loss $\Delta E(E, L)$ can be described as a function of gluon density: $\bar{n} = L/\lambda_g$, the mean number of jet scatterings, where L is the length traversed by the jet and λ_g is the mean free path in non-Abelian dense matter. In "thin plasma" approximation energy loss in first order is

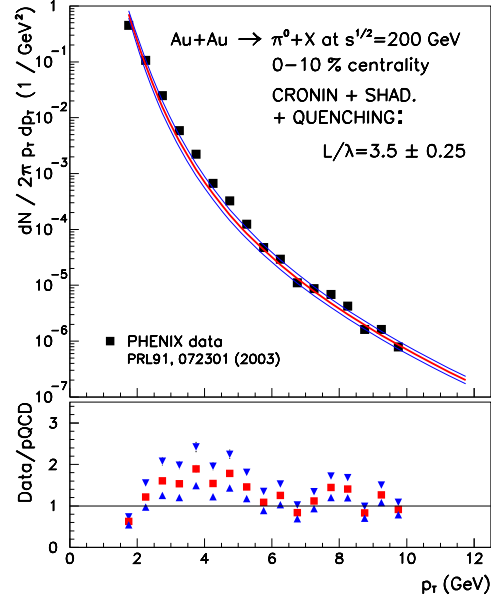


Fig. 1. Pion production in central $AuAu$ collision with the calculated opacities $\bar{n} = 3.5 \pm 0.25$ (upper panel). Data are from PHENIX Collaboration [1]. The lower panel displays a comparison between the data and the calculations.

given by the following form [7]:

$$\begin{aligned} \Delta E_{GLV}^{(1)} &= \frac{2C_R\alpha_s}{\pi} \frac{EL}{\lambda_g} \int_0^1 dx \int_0^{k_{max}^2} \frac{dk_T^2}{k_T^2} \times \\ &\times \int_0^{q_{max}^2} \frac{d^2\mathbf{q}_T \mu_{eff}^2}{\pi(\mathbf{q}_T^2 + \mu^2)^2} \cdot \frac{2\mathbf{k}_T \cdot \mathbf{q}_T (\mathbf{k} - \mathbf{q})_T^2 L^2}{16x^2 E^2 + (\mathbf{k} - \mathbf{q})_T^4 L^2} \\ &= \frac{C_R\alpha_s}{N(E)} \frac{L^2 \mu^2}{\lambda_g} \log\left(\frac{E}{\mu}\right), \end{aligned} \quad (4)$$

where C_R is the color Casimir of the jet, $\mu/\lambda_g \sim \alpha_s^2 \rho_{part}$ is a transport coefficient of the medium, proportional to the parton density, ρ_{part} . The color Debye screening scale is μ , and λ_g is the radiated gluon mean free path. $N(E)$ is an energy dependent factor with asymptotic value 4.

Considering a time-averaged, static plasma, the average energy loss, ΔE , will modify the argument of the FFs:

$$\frac{D_{\pi/c}(z_c, \tilde{Q}^2)}{\pi z_c^2} \rightarrow \frac{z_c^*}{z_c} \frac{D_{\pi/c}(z_c^*, \tilde{Q}^2)}{\pi z_c^2}. \quad (5)$$

Here $z_c^* = z_c / (1 - \Delta E/p_c)$ is the modified momentum fraction.

In Fig. 1 we present our result on pion production in most central (0 – 10%) $AuAu$ collisions at $\sqrt{s} = 200$ AGeV. We included all initial and final state effects discussed above and used the opacity value $\bar{n} = 3.5 \pm 0.25$ to reproduce the experimental data.

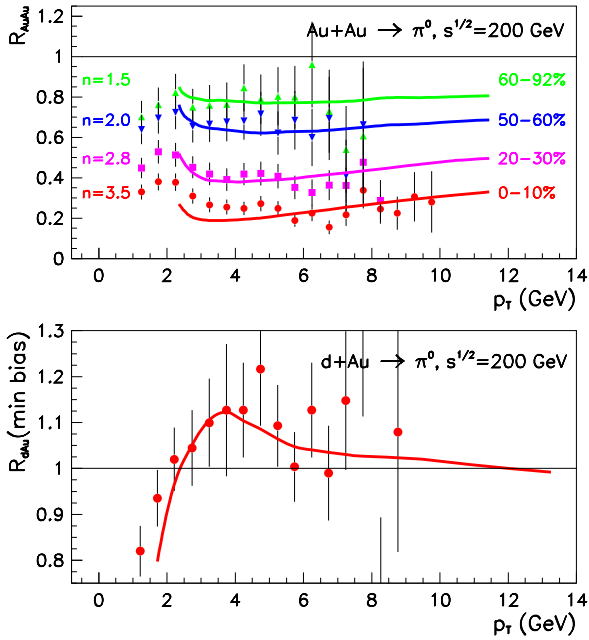


Fig. 2. Upper panel displays the pion production in $AuAu$ collision in different centrality bins with the calculated opacities. Data are from PHENIX Collaboration [1]. Lower panel shows the pion production in dAu collision [4] and the result of our calculation [15].

4 Centrality Dependence in $AuAu$ collisions

In the top panel of Fig. 2 we display the nuclear modification factor

$$R_{AA'}(p_T, b) = \frac{1}{N_{bin}} \cdot \frac{E_\pi d\sigma_\pi^{AA'}(b)/d^3p_T}{E_\pi d\sigma_\pi^{PP}/d^3p_T}, \quad (6)$$

(where N_{bin} is the number of binary collisions), as a function of p_T at different impact parameter ranges. The measured suppression is reproduced in the most central collisions with opacity $\bar{n} = 3.5 \pm 0.25$ as it was shown in Fig. 1. Curves with lower values of opacities are shown for comparison to the more peripheral data. Since the centrality 60–92% includes non-peripheral events, the obtained $\bar{n} = 1.5$ seems to be a reasonable opacity value for this bin. In the very peripheral case the opacity should be reduced to a small value [19], however $\pm 20\%$ error on the nuclear modification factor does not allow more detailed investigation. A more quantitative analysis can be performed, when data will be available with smaller error bars. At higher precision, the geometry of the hot overlap zone can be included and a more detailed analysis of the impact parameter dependence can be accomplished. In this case the properties of the produced hot matter will be studied in a more quantitative way.

In the bottom panel of Fig. 2 the dAu data are compared to our calculation [15] to demonstrate the validity of our description for the initial nuclear effects.

Acknowledgments

First of all, let us thank the Organizers and EPS for this informative meeting and the support of the participation of one of the authors (GGB). This work was supported in part by Hungarian grants T034842, T043455, T043514, U.S. DOE grant: DE-FG02-86ER40251, and NSF grant: INT0000211. Supercomputer time provided by BCPL in Norway and the EC – Access to Research Infrastructure action of the Improving Human Potential Programme is gratefully acknowledged.

References

1. G. David *et al.* (PHENIX Coll.), Nucl. Phys. **A698**, (2002) 227; D. d’Enterria *et al.* (PHENIX Coll.), Nucl. Phys. **A715**, (2003) 749; S.S. Adler *et al.* (PHENIX Coll.), Phys. Rev. Lett. **91**, (2003) 072301; (nucl-ex/0308006).
2. J.C. Dunlop *et al.* (STAR Coll.), Nucl. Phys. **A698**, (2002) 515; J.L. Klay *et al.* (STAR Coll.), Nucl. Phys. **A715**, (2003) 733; J. Adams *et al.* (STAR Coll.), Phys. Rev. Lett. **91**, (2003) 172302; (nucl-ex/0308023).
3. E. Wang, X.N. Wang, Phys. Rev. Lett. **89**, (2002) 162301; I. Vitev, M. Gyulassy, Phys. Rev. Lett. **89**, (2002) 252301; M. Gyulassy, P. Lévai, I. Vitev, Phys. Lett. **B538**, (2002) 282; M. Gyulassy, I. Vitev, X.N. Wang, B.W. Zhang, nucl-th/0302077.
4. S.S. Adler *et al.* (PHENIX Coll.), Phys. Rev. Lett. **91**, (2003) 072303.
5. J. Adams *et al.* (STAR Coll.), Phys. Rev. Lett. **91**, (2003) 072304.
6. M. Gyulassy and M. Plümer, Phys. Lett. **B243**, (1990) 432; M. Gyulassy, M. Plümer, M.H. Thoma and X.-N. Wang, Nucl. Phys. **A538**, (1992) 37c.
7. M. Gyulassy, P. Lévai and I. Vitev, Phys. Rev. Lett. **85**, (2000) 5535; Nucl. Phys. **B571**, (2000) 197; *ibid.* **B594**, (2001) 371.
8. C.Y. Wong and H. Wang, Phys. Rev. **C58**, (1998) 376.
9. X.N. Wang, Phys. Rev. **C61**, (2001) 064910.
10. Y. Zhang, G. Fai, G. Papp, G.G. Barnaföldi, and P. Lévai, Phys. Rev. **C65**, (2002) 034903.
11. G.G. Barnaföldi, P. Lévai, G. Papp, G. Fai, and Y. Zhang, APH NS Heavy Ion Phys. **18**, (2003) 79, nucl-th/0206006.
12. G. Papp, G.G. Barnaföldi, P. Lévai, and G. Fai, hep-ph/0212249.
13. F. Aversa, P. Chiappetta, M. Greco, and J.Ph. Guillet, Nucl. Phys. **B327**, (1989) 105.
14. P. Aurenche, M. Fontannaz, J.Ph. Guillet, B. Kniehl, E. Pilon, and M. Werlen, Eur. Phys. J. **C9**, (1999) 109; P. Aurenche, M. Fontannaz, J.Ph. Guillet, B. Kniehl, and M. Werlen, Eur. Phys. J. **C13**, (2001) 347.
15. P. Lévai, G. Papp, G.G. Barnaföldi and G. Fai, nucl-th/0306019.
16. A.D. Martin, R.G. Roberts, W.J. Stirling, and R.S. Thorne, Eur. Phys. J. **C23**, (2002) 73.
17. S.J. Li and X.N. Wang, Phys. Lett. **B527**, (2002) 85.
18. B.A. Kniehl, G. Kramer and B. Pötter, Nucl. Phys. **B597**, (2001) 337, hep-ph/0011155.
19. G.G. Barnaföldi, P. Lévai, G. Papp, G. Fai, and Y. Zhang, *Proc. of XXXII. Int. Symposium on Multiparticle Dynamics*, (World Sci. Singapore 2003), nucl-th/0212111.